Asymptotic regimes of ridge and rift formation in a thin viscous sheet model

Carlos Alberto Perazzo and Julio Gratton

Citation: Physics of Fluids (1994-present) **20**, 043103 (2008); doi: 10.1063/1.2908356
View online: http://dx.doi.org/10.1063/1.2908356
View Table of Contents: http://scitation.aip.org/content/aip/journal/pof2/20/4?ver=pdfcov
Published by the AIP Publishing

Asymptotic regimes of ridge and rift formation in a thin viscous sheet model

Carlos Alberto Perazzo[1,a)] and Julio Gratton[2,b)]
[1]*Universidad Favaloro, Solís 453, 1078 Buenos Aires, Argentina*
[2]*INFIP-CONICET, Dto. de Física, Facultad de Ciencias Exactas y Naturales, Universidad de Buenos Aires, Ciudad Universitaria, Pab. I, 1428 Buenos Aires, Argentina*

(Received 13 December 2007; accepted 24 March 2008; published online 28 April 2008)

We numerically and theoretically investigate the evolution of the ridges and rifts produced by the convergent and divergent motions of two substrates over which an initially uniform layer of a Newtonian liquid rests. We put particular emphasis on the various asymptotic self-similar and quasi-self-similar regimes that occur in these processes. During the growth of a ridge, two self-similar stages occur; the first takes place in the initial linear phase, and the second is obtained for a large time. Initially, the width and the height of the ridge increase as $t^{1/2}$. For a very large time, the width grows as $t^{3/4}$, while the height increases as $t^{1/4}$. On the other hand, in the process of formation of a rift, there are three self-similar asymptotics. The initial linear phase is similar to that for ridges. The second stage corresponds to the separation of the current in two parts, leaving a dry region in between. Last, for a very large t, each of the two parts in which the current has separated approaches the self-similar viscous dam break solution. © *2008 American Institute of Physics*.
[DOI: 10.1063/1.2908356]

I. INTRODUCTION

Viscous gravity currents in which inertia is negligible and viscous stresses balance the gravity force are common in nature as well as in man-made situations. In many instances, the thickness of these currents is small compared to their horizontal extension, so that they can be described by means of the lubrication approximation.[1] The specific problems we consider in this paper are the evolution of the ridges and rifts produced by the convergent and divergent motions of two substrates over which an initially uniform layer of a Newtonian liquid rests. The formation of a ridge has been investigated theoretically and with a laboratory model,[2] and numerically[3,4] because of its connection with the process of mountain building. The theoretical model that is the basis of these investigations belongs to the class of the so called thin sheet models,[5] which have been extensively employed to study the deformations of the continental lithosphere mainly by means of numerical simulations. A classification of these models was given by Medvedev and Podladchikov.[6] The fluid mechanics involved in several geophysical problems has been discussed by Huppert.[7–9]

In a previous paper[10] by Gratton, the scaling laws for the evolution of the height and width of a mountain belt were derived by means of dimensional analysis, with physical assumptions essentially equivalent to those of the model of Buck and Sokoutis.[2] We shall not present details that the reader can find in many papers such as that by Rey *et al.*[11] since it is not the purpose of this paper to investigate mountain building. Our aim is to achieve a better basic understanding of the fluid mechanics involved in the evolution of the ridges and rifts produced by viscous flows, with particular emphasis on the various asymptotic self-similar and quasi-self-similar regimes that occur in these processes.

This paper is divided into five parts. In the next section, we derive the governing equations of the viscous flows for a symmetric convergent or divergent motion of the substrates. In Sec. III, we discuss the numerical solutions obtained by means of a finite difference method. In Sec. IV, we investigate the behavior of the solution close to the beginning of the process, when the governing equations can be linearized. We find that a self-similar regime occurs in this stage, during which the width and the height (depth) of the ridge (rift) scale as $t^{1/2}$. In Sec. V, we investigate the remaining self-similar and quasi-self-similar asymptotics that occur in other space-time domains for ridges as well as for rifts. In Sec. VI, we show that some of the results reported in the previous sections can be generalized to the case when the substrates move nonsymmetrically. Final comments are presented in Sec. VII.

II. GOVERNING EQUATIONS

Consider a uniform liquid film with thickness H_0 that rests on a horizontal rigid surface, which is divided into two parts at $X=0$. At $T=0$, both parts start to converge or diverge with the same constant speed U_0, producing a ridge or a rift, respectively (see Fig. 1). Due to the symmetry of the problem, it is sufficient to consider only the half-plane $X>0$ and imagine that at $X=0$, there is a vertical impermeable wall along which the liquid slips. We define the velocity of the substrate as σU_0 (here, $U_0>0$ and $\sigma=\pm 1$). Then, if $\sigma=1$, the substrate is moving to the right, away from the wall, so that a rift is formed. If $\sigma=-1$ the substrate moves to the left, accumulating the fluid against the wall, thus producing a

[a)]Electronic mail: perazzo@favaloro.edu.ar.
[b)]Electronic mail: jgratton@tinfip.lfp.uba.ar.

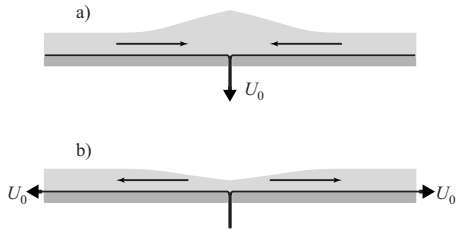

FIG. 1. Formation of ridges and rifts. (a) Due to the convergent movement of the substrate, the fluid accumulates in the region of convergence generating a ridge. (b) Due to the divergent movement of the substrate, the fluid leaves the region of divergence generating a rift.

ridge. We shall assume a slow viscosity-dominated flow and we shall employ a slight generalization of the well-known lubrication approximation (see, for example, Refs. 1 and 12–14) to take into account the motion of the substrate. Let $H \equiv H(X,T)$ be the thickness of the liquid. We assume that the slope of the free surface is gentle, so that the horizontal component V of the velocity of the fluid is much larger than the vertical one and that the vertical gradient of V is much larger than the horizontal gradient. In this way, the Stokes equation takes the form

$$0 = -\frac{1}{\rho}\frac{\partial P}{\partial X} + \nu\frac{\partial^2 V}{\partial Z^2},$$
$$0 = -\frac{\partial P}{\partial Z} - \rho g, \tag{1}$$

where P is the pressure, g is the acceleration of gravity, ρ is the density, and ν is the kinematic viscosity. From the last equation, one obtains that the pressure is hydrostatic, and by replacing P in the first one, integrating twice, and imposing the no stress condition $\partial V/\partial Z=0$ at $Z=H(X,T)$ and the no slip condition $V=\sigma U_0$ at the substrate, one obtains

$$V = \sigma U_0 - \frac{g}{\nu}\frac{\partial H}{\partial X}\left(ZH - \frac{1}{2}Z^2\right). \tag{2}$$

We define $U \equiv U(X,T)$ as the vertical average of V, so that

$$U = \sigma U_0 - \frac{g}{3\nu}\frac{\partial H}{\partial X}H^2. \tag{3}$$

By using the continuity equation, we finally obtain

$$\frac{\partial H}{\partial T} = -\sigma U_0\frac{\partial H}{\partial X} + \frac{g}{3\nu}\frac{\partial}{\partial X}\left(H^3\frac{\partial H}{\partial X}\right). \tag{4}$$

We define the dimensionless variables u, h, x, and t by means of

$$U = U_0 u, \quad H = H_0 h,$$
$$X = \frac{g}{3\nu}\frac{H_0^3}{U_0}x, \quad T = \frac{g}{3\nu}\frac{H_0^3}{U_0^2}t, \tag{5}$$

so that Eq. (4) takes the form

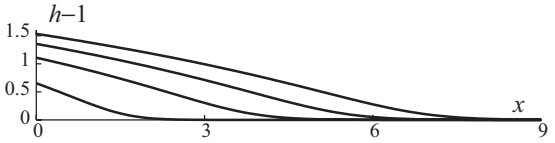

FIG. 2. Numerical profiles of a ridge for $t=0.6$, 2.4, 4.2, and 6.

$$\frac{\partial h}{\partial t} = -\sigma\frac{\partial h}{\partial x} + \frac{\partial}{\partial x}\left(h^3\frac{\partial h}{\partial x}\right), \tag{6}$$

and from Eq. (3), the connection between u and h is given by

$$u = \sigma - h^2\frac{\partial h}{\partial x}. \tag{7}$$

We solve Eq. (6) in the domain $x \geq 0$ starting from the initial condition $h(x,0)=1$. Since u must be continuous at $x=0$ and the motion of the substrates is symmetric, we must require $u(0,t)=0$, which implies

$$h^2\left.\frac{\partial h}{\partial x}\right|_{x=0} = \sigma. \tag{8}$$

This boundary condition holds provided there are no sources nor sinks at $x=0$ and only if the motion of the substrates is symmetric [the appropriate boundary condition for the nonsymmetric convergent motion of the substrates is given by Eq. (26)]. In Eqs. (6)–(8), $\sigma=1$ for rift formation and $\sigma=-1$ for ridge formation. Notice that the conservation of mass implies that $\int_0^\infty h_t dx = -\sigma$.

III. NUMERICAL SOLUTIONS

Problems (6)–(8) do not admit closed form solutions so that they must be solved numerically. To this purpose, we used a second order implicit finite difference scheme.[15]

Some results for ridge formation are shown in Fig. 2. It can be seen that h has an inflection point that is located near $x=0$ at the beginning and moves toward large x as t increases, tending to reach the leading part of the ridge, where h approaches 1. It can be also noticed that the aspect ratio (height/width) of the ridge diminishes with time. This occurs because as the ridge grows, its width increases more rapidly since the diffusion term of Eq. (6) scales as h^4. The evolution of $h_w \equiv h(0,t)$ is shown in Figs. 3 and 4.

Results for rifts are shown in Figs. 5 and 6. As t increases, h_w rapidly decreases and vanishes at a certain time $t_s=0.1786$. At this moment, the current separates into two parts, and for $t>t_s$, there is a dry region that extends from $x=0$ to a front located at $x_f(t)$; thus, $h(x,t>t_s)=0$ for $0 \leq x < x_f(t)$. For $t>t_s$, the boundary condition (8) no longer applies.

To our knowledge, the separation predicted by the numerical solution has not been observed yet and the present problem still awaits investigation in the laboratory. However, it is reasonable that separation will actually occur for a divergent motion of the substrates. The average flow uh is a combination of the effect of the motion of the substrate that tends to carry the fluid to the right [the first term in the right hand side of Eq. (7)], thus lowering h near $x=0$, and of the

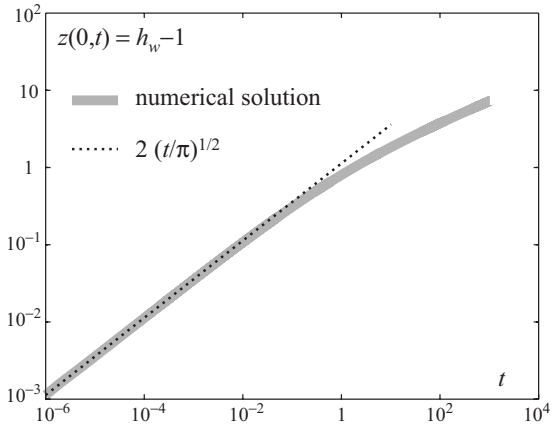

FIG. 3. Maximum height of a ridge. The thick line corresponds to the numerical results and the dashed line corresponds to the scaling law given by the self-similar solution (11).

effect of the gravity spreading [the second term in the right hand side of (7)] that tends to keep h uniform. The first effect prevails everywhere (except only at $x=0$ where both effects are exactly balanced), so that h_w decreases with time. It will be shown later that as h_w becomes very small, the flow approaches an asymptotic self-similar regime for which h_w vanishes at a finite t_s. After this has happened, the current has a front that is carried to the right by the motion of the substrate. As we will show later, immediately after t_s, the motion close to the front is also self-similar. These results follow from the lubrication approximation in which we have neglected surface effects and from our assumption that the velocity of the substrates is discontinuous at $x=0$. We believe that the inclusion of surface effects will certainly modify the phenomenon, but we expect that some sort of separation will also happen, eventually with more complex topological changes, like the production of droplets (as occurs in situations involving dewetting). On the other hand, if the velocity of the substrates is assumed to change smoothly on a small interval δx centered at $x=0$, we believe that a small quantity of liquid, which vanishes as $t \to \infty$, will remain inside this

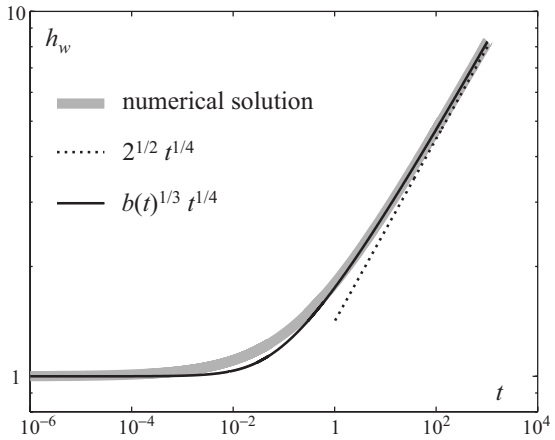

FIG. 4. Maximum height of a ridge. The thick line is the numerical result, the thin line is calculated from Eq. (20), and the dashed line is from Eq. (18).

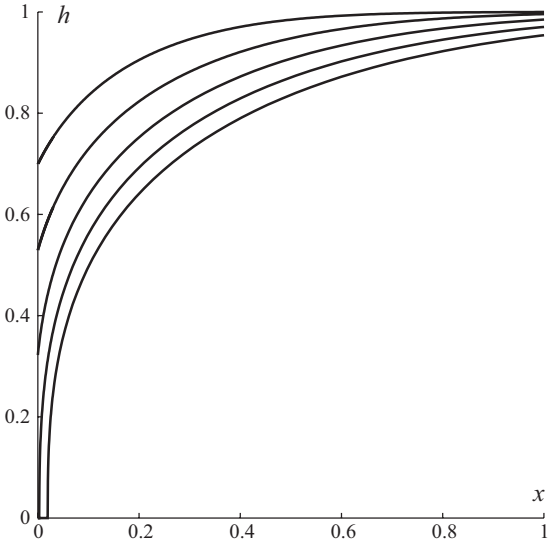

FIG. 5. Numerical profiles of a rift for $t=0.05$, 0.1, 0.15, 0.2, and 0.25.

interval, so that, strictly speaking, no separation will take place.

IV. LINEAR REGIME

For small t, when h is close to 1, we can write $h=1-\sigma z$ with $z \ll 1$, thus allowing to linearize Eqs. (6) and (8), which reduce to

$$\frac{\partial z}{\partial t} = -\sigma \frac{\partial z}{\partial x} + \frac{\partial^2 z}{\partial x^2}, \qquad \left.\frac{\partial z}{\partial x}\right|_{x=0} = -1. \tag{9}$$

The solution of these equations (for details, see the Appendix) for a ridge ($\sigma=-1$) and for a rift ($\sigma=1$) is given by

$$z = -\sigma \frac{e^{-s^2}}{\sqrt{\pi}} \left[2\sqrt{t} H_{-2}(s) + \sum_{j=1}^{\infty} (2\sqrt{t})^j H_{-1-j}(s) \right], \tag{10}$$

where $s=(t-\sigma x)/2\sqrt{t}$ and $H_q(s)$ denotes the Hermite

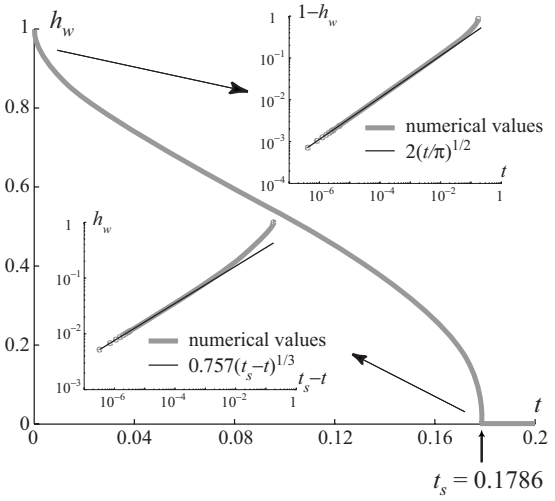

FIG. 6. Minimum height of a rift. The insets show the behavior close to $t=0$ and to $t=t_s$.

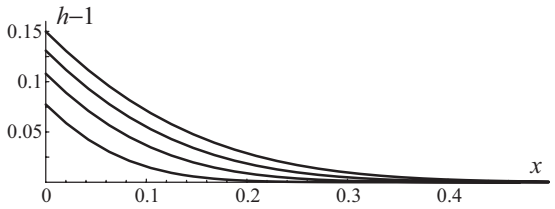

FIG. 7. Analytical solution (10) of the linearized problem for $t=0.005$, 0.01, 0.015, and 0.02.

function of order q. Notice that this approximate solution does not conserve the mass since $\int_0^\infty z_t dx = 1+\sigma z(0,t) \neq 1$.

In Fig. 7, we show the z profiles (for $\sigma=-1$) for different times. Notice that within this approximation, the solutions for a rift and a ridge are symmetric around the axis $h=1$.

These solutions are not self-similar, but tend to self-similarity for $t\to 0$. To see this, we seek solutions of Eq. (9) of the form $z=t^{1/2}f(\psi)$ with $\psi=x/2\sqrt{t}$. By substituting this into Eq. (9), one obtains

$$f'' + 2(\psi - \sigma t^{1/2})f' - 2f = 0, \quad f'(0) = -2.$$

Here and in what follows, primes denote derivatives with respect to the argument. For small t, we can neglect the term proportional to $t^{1/2}$ (this implies $x \gg 2t$). Then, the solution that is bounded for $z\to\infty$ is

$$z_s = 2\sqrt{t}\left[\frac{e^{-\psi^2}}{\sqrt{\pi}} - \psi\,\mathrm{erfc}(\psi)\right], \tag{11}$$

where $\mathrm{erfc}(\psi)$ is the complementary error function. In Fig. 3, it can be seen that for a small time, $z(0,t)$ tends to the self-similar behavior $z_s(0,t)=2\sqrt{t/\pi}$. In this regime, the height (depth) and the width of the ridge (rift) increase as $t^{1/2}$, so that the aspect ratio is constant while the area of the cross section increases as t.

V. SELF-SIMILAR AND QUASI-SELF-SIMILAR REGIMES

To find the self-similar solutions of the full nonlinear problem (6) and (8), we assume h of the form[16]

$$h = t^\alpha f(\xi), \quad \xi = x t^{-\beta}. \tag{12}$$

By substituting in Eqs. (6) and (8), one finds

$$\alpha f - \beta\xi f' = t^{1-\beta}[-\sigma f + t^{3\alpha-\beta} f^3 f']', \quad f^2 f'|_{\xi=0} = \sigma t^{\beta-3\alpha}. \tag{13}$$

The initial condition $h(x,0)=1$ and the condition $h(\infty,t)=1$ both require

$$f(\infty) = t^{-\alpha}. \tag{14}$$

Finally, mass conservation implies

$$\int_0^\infty (\alpha f - \beta\xi f')d\xi = t^{1-\alpha-\beta}.$$

Since f depends on t only through ξ, the variable t must disappear from the preceding formulas. This is not possible in general, but it can be approximately achieved in certain spatial and/or temporal domains. Then, to go further, we must specify the type of self-similar solution we are seeking.

A. Self-similar and quasi-self-similar regimes in ridge formation

Now, we look for a self-similar regime for large t and small x, so that this regime has to satisfy the conservation of mass and the boundary condition at $\xi=0$. These two conditions imply $\alpha=1/4$ and $\beta=3/4$. With these exponents, the leading term of Eq. (13) can be integrated once to obtain

$$f^3 f' + f = A = \text{const}. \tag{15}$$

By comparing this with the boundary condition at $\xi=0$, we find that $A=0$. Then, the solution of Eq. (15) is

$$f = \begin{cases} (b-3\xi)^{1/3} & \text{if } \xi < b/3 \\ 0 & \text{if } \xi > b/3, \end{cases} \tag{16}$$

where $b=$const. This solution has a front at $\xi=b/3$. From the mass conservation between $\xi=0$ and $\xi=b/3$, we obtain $b=\sqrt{8}$. From this, we find the self-similar solution for $t\gg 1$ as

$$h_s = h_w\left(1-\frac{x}{x_f}\right)^{1/3} \quad \text{if } x<x_f, \quad 0 \text{ if } x>x_f, \tag{17}$$

where

$$h_w = \sqrt{2}t^{1/4}, \quad x_f = \frac{\sqrt{8}}{3}t^{3/4}. \tag{18}$$

In Fig. 4, we compare the preceding expression of h_w to the numerical result to see how this self-similar regime is approached.

A better approximation can be achieved by means of the quasi-self-similarity approach.[17–21] To this purpose, we allow the integration constant b to depend weakly on time. The justification of this procedure was clearly presented by Bertsch *et al.*[21] Accordingly, we require that the mass added to the ridge appears above $h=1$ (i.e., for $f \geqslant t^{-1/4}$). Then, the conservation of mass implies

$$\int_0^{\xi_a} (f - 3\xi f')d\xi = 4,$$

where $\xi_a=(b-t^{-3/4})/3$ is the place where $h=1$. One then finds a quasi-self-similar solution of the form

$$h_q = h_w\left(1-\frac{x}{x_f}\right)^{1/3} \quad \text{if } x<a, \quad h_q = 1 \text{ if } x>a. \tag{19}$$

Here, $a=x_f-1/3$ is the half-width of the ridge, and h_w and x_f are given by

$$h_w = b(t)^{1/3}t^{1/4}, \quad x_f = \tfrac{1}{3}b(t)t^{3/4}, \tag{20}$$

where b is the positive real root of the polynomial $b^4-(4+bt^{-1/4})^3$.

It can be observed in Fig. 4 that the maximum height given by h_q agrees much better with the numerical results than that given by h_s. Actually, $h_q(0,t)$ never differs from the numerical values by more than 8% for any t. In Fig. 8, we compare the numerical solutions for large times to the quasi-self-similar solution h_q. The quasi-self-similar solution de-

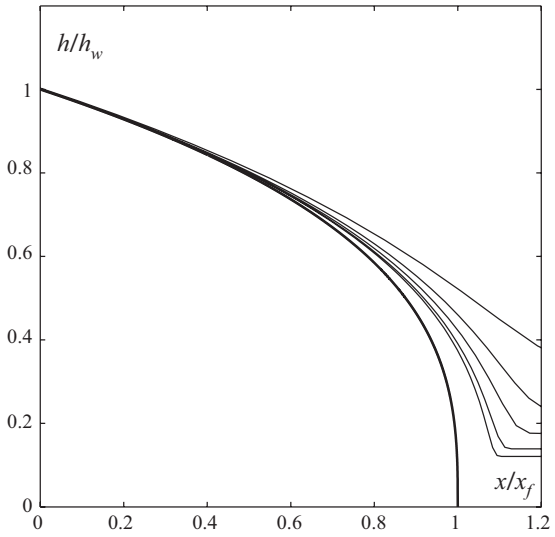

FIG. 8. Comparison of the quasi-self-similar solutions (19) and (20) (thick line) with the numerical solutions for $t=18$, 78, 216, 576, and 1026 (thin lines).

scribes very well the large time behavior near the crest of the ridge, but not so well far from the crest where $h(x,t)$ is close to 1. This should be expected since the quasi-self-similar regime does not verify condition (14).

To obtain a better description far from the crest, we follow a similar approach as before, that is, we look for a solution that satisfies condition (14), sacrificing the condition at $\xi=0$. As before, we set $\alpha=1/4$, $\beta=3/4$ and integrate the leading term of the differential equation for f. The result is again Eq. (15) but now $A\neq 0$ and the solution of Eq. (15) is given in implicit form by

$$\xi = -\frac{1}{3}f^3 - \frac{A}{2}f^2 - A^2 f - A^3 \ln(f-A) + c, \tag{21}$$

with $c=$const. Now, we allow the integration constants A and c to weakly depend on t. To satisfy Eq. (14), we set $A=t^{-1/4}$, and to determine c, we require that when $x=0$, $h=h_w$. The solution is then

$$x = \frac{1}{3}(h_w^3 - h^3) + \frac{1}{2}(h_w^2 - h^2) + (h_w - h) + \ln\left(\frac{h_w - 1}{h-1}\right). \tag{22}$$

Solutions of this kind have been found in other contexts, for example, as the large time asymptotic of a current produced by a piston that is pushing a viscous layer.[13] In the previous expression, we have not yet specified h_w. The logical choice is expression (20), which describes very well the time behavior at the crest, but this improvement is not sufficient because the solution so obtained does not satisfy yet the boundary condition at $x=0$ (except in the limit $t\to\infty$). Fortunately, it can be shown that it is possible to modify Eq. (22) in such a way as to fulfill this condition. By omitting details, the idea is to rescale ξ in Eq. (15) to ensure that $f'(0)$ has the appropriate value. The necessary scaling factor is found to be $f(0)/[f(0)-A]$. This implies that we must rescale x by multiplying the right hand side of Eq. (22) by the factor $(h_w-1)/h_w$. In Fig. 9, we compare the numerical profiles at different times to the profiles given by the rescaled solution (22), in which h_w is given by Eq. (20). It can be observed that the agreement is excellent even for times that are not very large.

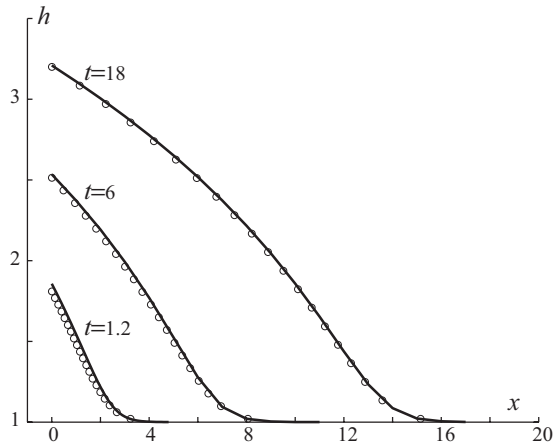

FIG. 9. Comparison of the numerical profiles (lines) at different times with the profiles of the rescaled solution (circles) from Eq. (22) in which h_w is given by Eq. (20).

B. Self-similar regimes in rift formation

Since the self-similar regime for very small t has been discussed before, we shall deal here with the self-similar regimes that occur in later stages of the process.

1. The behavior at separation

As previously mentioned, the minimum height of a rift decreases rapidly and vanishes at t_s, so that $h\ll 1$ for $|x|\ll 1$ and $t'\equiv|t-t_s|\ll 1$ (see Figs. 5 and 6). Then, in this domain, there is no scale for h. We then expect a self-similar regime in which the dimensional height H does not depend on H_0. From Eqs. (5) and (12), it is clear that such a regime requires $\alpha=\frac{1}{3}$ and $\beta=1$ [this pair of values is the only one for which Eq. (13) does not depend on time]. Then,

$$h = t'^{1/3} f(\xi), \tag{23}$$

where now $\xi=x/t'$. In the lower inset of Fig. 6, we compare the numerical results with the scaling law for h_w predicted by this type of self-similarity.

By replacing Eq. (23) in Eq. (6), we obtain

$$\tfrac{1}{3}f - \xi f' = \mp(-f + f^3 f')', \tag{24}$$

where the $-$ sign is for $t<t_s$ and the $+$ sign is for $t>t_s$. To integrate Eq. (24) for $t<t_s$, we only need the value of $f(0)$ [then $f'(0)$ is determined by the boundary condition $f^2f'=1$ at $\xi=0$]. To this purpose, we notice from the lower inset of Fig. 6 that $h_w=0.757t'^{1/3}$; then, by comparing this with Eq. (23), we find $f(0)=0.757$. To integrate Eq. (24) for $t>t_s$, we notice that according to Eq. (7), we need $h\propto|x-x_f|^{1/3}$ to have a front that moves with a finite nonzero velocity with respect to the substrate. Then, by using Eq. (23), we find that near the front, $f=k(\xi-\xi_f)^{1/3}$, where ξ_f is the self-similar coordinate of the front and k is a constant. To find k, we notice that

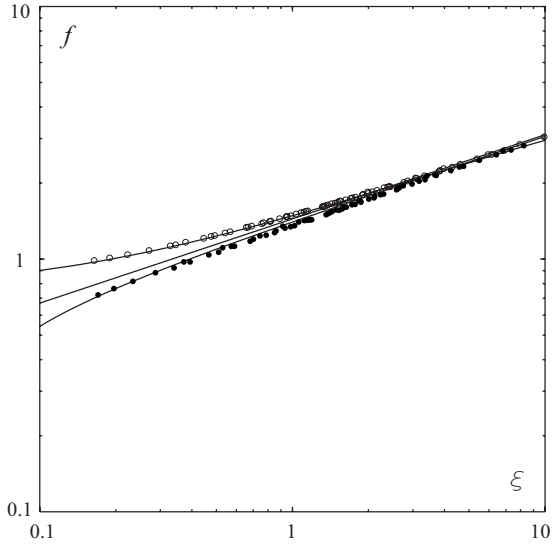

FIG. 10. Self-similar behavior near separation. The circles are points with coordinates $[x/|t-t_s|, h(x,t)/|t-t_s|^{1/3}]$ calculated from the numerical solutions of the PDE (6) with boundary condition (8) for $\sigma=1$. For each of the eight numerical $h(x,t)$ profiles immediately before separation (open circles) and for each of the eight numerical $h(x,t)$ profiles immediately after separation (filled circles), we plot the points that fall within the range $0.1 \leqslant \xi \leqslant 10$. The lines are the solutions of the ODE (24) with the initial conditions described in the text; the straight line is the solution $h=(3x)^{1/3}$. The fact that the circles are located almost over the lines indicates that problems (6) and (8) develop the self-similar regime defined by Eq. (23) with f determined by Eq. (24) near $x=0$ and $t=t_s$.

before separation and for small x, the profile $h(x,t)$ approaches $(3x)^{1/3}$ for $t \to t_s$. Then, it seems reasonable to assume that $h(x,t)=(3x)^{1/3}$ for $t=t_s$ and small x since we see no reason why an abrupt change in the shape of the profile of the current should occur at this moment. On the other hand, the moment $t=t_s$ and finite x corresponds to $\xi \to \infty$, so that near the front, $f \to k\xi^{1/3}$. Then, for $t>t_s$ to avoid as before abrupt changes in the behavior for which we see no reason, we require $k=3^{1/3}$. With this value of k and a value of ξ_s, we employ the form of f near a front to start the numerical integration of the ordinary differential equation (ODE) (24), using ξ_f as a fitting parameter.

In Fig. 10, we compare the (numerical) solutions of these equations with our numerical solutions of Eq. (6) for t close to t_s and small x. The best fit with the numerical solutions of the partial differential equation (PDE) (6) is achieved with $\xi_f=0.045$. It can be appreciated that there is excellent agreement between the numerical solutions of the PDE and the self-similar regimes obtained from Eqs. (23) and (24), a fact that incidentally validates our numerical finite difference scheme.

2. Large time behavior

For very large t, h tends to the solution of the viscous dam break problem,[13] as seen by an observer moving with velocity $-U_0$. This solution is self-similar and in this reference frame has the form $h=f(x'/\xi_f\sqrt{t})$, where $x'=x-U_0t$ and $\xi_f=-0.492\cdots$. There is no closed form for f. In Fig. 11, we can observe this solution.

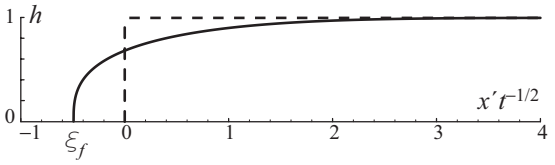

FIG. 11. Self-similar solution of the viscous dam break problem.

VI. ASYMMETRIC MOTION OF THE SUBSTRATES

A simple generalization of the problem studied before is to assume that the velocities of the two parts of the substrate are different. For definiteness, we shall consider only the formation of a ridge. Let us assume that the left part of the substrate in Fig. 1 moves with a velocity $U_0>0$ and the right half with a velocity $-\mu U_0<0$, where $0 \leqslant \mu \leqslant 1$ quantifies the asymmetry. This means that the influx of mass coming from the left is larger than that arriving from the right. The dimensionless variables are defined as in Eq. (5). Then, Eq. (6) (with $\sigma=1$) holds for $x \leqslant 0$, but for $x \geqslant 0$ we have

$$\frac{\partial h}{\partial t} = \mu \frac{\partial h}{\partial x} + \frac{\partial}{\partial x}\left(h^3 \frac{\partial h}{\partial x}\right). \tag{25}$$

At $x=0$, the height h is continuous, but $\partial h/\partial x$ has a discontinuity given by

$$\left.\frac{\partial h}{\partial x}\right|_{x\to 0^-} - \left.\frac{\partial h}{\partial x}\right|_{x\to 0^+} = \frac{1+\mu}{h(0,t)^2}. \tag{26}$$

This condition implies that at $x=0$, there is mass flowing from the left to the right, which did not happen in the symmetric case.

In the asymmetric case for a given μ, Eqs. (6) and (25) must be solved in $x \leqslant 0$ and $x \geqslant 0$, respectively, starting from the initial condition $h(x,0)=1$ and subject to the matching condition (26). Notice that now the conservation of mass implies $\int_{-\infty}^{\infty} h_t dx = 1+\mu$.

We now give the main results, omitting details for brevity.

- The crest of the ridge remains at $x=0$ for all t.
- In the linear self-similar regime (small t), the ridge is symmetric around $x=0$ independently of μ, and its width and height scale as $t^{1/2}$. The solution for $x>0$ is given by Eq. (11) with the factor 2 replaced by $1+\mu$. For $x<0$ is its specular image.
- For larger t, the ridge becomes asymmetric, being narrower and steeper for $x<0$.
- For t very large and $0<\mu \leqslant 1$, a self-similar asymptotic of the same kind as Eqs. (17) and (18) develops. The profile of the ridge is asymmetric, but its height and width scale as $t^{1/4}$ and $t^{3/4}$, respectively.
- The case $\mu=0$ is different. As t grows, the $x>0$ portion of the ridge becomes increasingly dominant, and its height and width scale as $t^{1/5}$ and $t^{4/5}$, respectively.

It should be mentioned that Buck and Sokoutis[2] investigated the self-similar regime that appears for small t in the linearized problem for the case $\mu=0$. They obtained the $t^{1/2}$

scaling for the width and height of the ridge, but they give a wrong formula for z that does not satisfy the differential equation.

VII. FINAL COMMENTS

From Figs. 3 and 4 it can be observed that during the growth of a ridge, two self-similar stages occur. In the initial linear stage, the profile h is given by the self-similar solution (11). Later on, h is described by the self-similar solutions (17) and (18) and even better by the quasi-self-similar solutions (19) and (20). The transition between these stages occurs for t of the order of unity and corresponds to the migration of the inflection point of h, which is initially very close to $x=0$, while for $t\to\infty$, it approaches x_f. During the linear phase, both the width and the height of the ridge increase as $t^{1/2}$. As the height increases, the lateral spreading becomes dominant, so that most of the mass accumulated in the ridge increases its width, which grows as $t^{3/4}$, much faster than its height, which increases as $t^{1/4}$. These scalings agree with those obtained in the context of the growth of mountain belts.[10] The peak of the ridge always remains at $x=0$ even if the motion of the substrates is not symmetrical. The shape of the ridge is symmetrical during the linear stage, regardless of μ, but for later times, it becomes asymmetrical for $\mu\neq 1$. The scaling laws we obtained in the symmetric case for both stages are also obtained in the nonsymmetric case, except for $\mu=0$.

On the other hand, in the formation of a rift, there are three spatiotemporal domains, in which self-similar asymptotics develop. The initial linear stage is the same as for ridges, with a change of sign of z. The second domain occurs close to $x=0$ and near $t=t_s$, where the separation of the current into two parts leaving a dry region in between takes place. In this domain, there is a self-similar regime in which h_w scales as $|t-t_s|^{1/3}$ and the width of the dry region grows as $|t-t_s|$. Last, for very large t, each of the two parts in which the current has separated approaches the self-similar viscous dam break solution.

ACKNOWLEDGMENTS

We acknowledge Grant No. PIP 5377 of the CONICET, Grant No. X031 of the University of Buenos Aires, Grant No. PICTR 2002-00094 of the ANPCYT, and Grant No. PICTO FONCYT/UF 21360 BID OC/AR 1728 from FONCYT and Universidad Favaloro.

APPENDIX: LINEARIZED SOLUTION

To find the solution of Eq. (9), we define $\theta=t-\sigma x$ and set $z(x,t)=\phi(\theta,t)$ in Eq. (9) to obtain

$$\frac{\partial\phi}{\partial t}=\frac{\partial^2\phi}{\partial\theta^2},\qquad \left.\frac{\partial\phi}{\partial\theta}\right|_{\theta=t}=\sigma. \tag{A1}$$

Due to the peculiar boundary condition at $\theta=t$, the usual methods to solve the heat diffusion equation cannot be used. We assume $\phi=f(t)g(t,\theta)$, substitute in the first equation of Eq. (A1), and divide by fg to find

$$\frac{f'}{f}=\frac{1}{g}\left(\frac{\partial^2 g}{\partial\theta^2}-\frac{\partial g}{\partial t}\right), \tag{A2}$$

which implies that the right hand side depends only on t. By assuming $g=g(w)$ with $w=\theta/\sqrt{t}$ and integrating, one finds

$$g''+\tfrac{1}{2}wg'=Kg,\quad K=\text{const}. \tag{A3}$$

If $K=0$, one obtains from Eq. (A3) the familiar self-similar point source solution of heat diffusion. If $K\neq 0$, the general solution of Eq. (A3) can be expressed in terms of a linear combination of Hermite functions and confluent hypergeometric functions. In the present case, we must discard the hypergeometric functions as they diverge for large x. On the other hand, the solution for f is $f=At^K$, $A=$const. Then, it can be shown that the solution that satisfies the boundary condition (A1) is given by the series

$$\phi=-\sigma\frac{e^{-\theta^2/4t}}{\sqrt{\pi}}\left[2\sqrt{t}H_{-2}\left(\frac{\theta}{2\sqrt{t}}\right)+\sum_{j=1}^{\infty}(2\sqrt{t})^j H_{-1-j}\left(\frac{\theta}{2\sqrt{t}}\right)\right]. \tag{A4}$$

[1] J. D. Buckmaster, "Viscous sheets advancing over dry beds," J. Fluid Mech. **81**, 735 (1977).
[2] W. R. Buck and D. Sokoutis, "Analogue model of gravitational collapse and surface extension during continental convergence," Nature (London) **369**, 737 (1994).
[3] S. Medvedev, "Mechanics of viscous wedges: Modeling by analytical and numerical approaches," J. Geophys. Res. **107**, 2123, DOI: 10.1029/2001JB000145 (2002).
[4] S. D. Willett, "Rheological dependence of extension in wedge models of convergent orogens," Tectonophysics **305**, 419 (1999).
[5] P. C. England and D. P. McKenzie, "A thin viscous sheet model for continental deformation," Geophys. J. R. Astron. Soc. **70**, 295 (1982).
[6] S. E. Medvedev and Y. Y. Podladchikov, "New extended thin-sheet approximation for geodynamic applications. I. Model formulation," Geophys. J. Int. **136**, 567 (1999).
[7] H. E. Huppert, "The intrusion of fluid mechanics into geology," J. Fluid Mech. **173**, 557 (1986).
[8] H. E. Huppert, in *Perspectives in Fluid Dynamics: A Collective Introduction to Current Research*, edited by G. K. Batchelor, H. K. Moffatt, and M. G. Worster (Cambridge University Press, Cambridge, 2003), Chap. 9, pp. 447–506.
[9] H. E. Huppert, "Gravity currents: A personal perspective," J. Fluid Mech. **554**, 299 (2006).
[10] J. Gratton, "Crustal shortening, root spreading, isostasy, and the growth of orogenic belts: A dimensional analysis," J. Geophys. Res. **94**, 15627, DOI: 10.1029/JB094iB11p15627 (1989).
[11] P. Rey, O. Vanderhaeghe, and C. Teyssier, "Gravitational collapse of the continental crust: Definition, regimes and modes," Tectonophysics **342**, 435 (2001).
[12] H. E. Huppert, "The propagation of two-dimensional and axisymmetric viscous gravity currents over a rigid horizontal surface," J. Fluid Mech. **121**, 43 (1982).
[13] J. Gratton and F. Minotti, "Self-similar viscous gravity currents: Phase-plane formalism," J. Fluid Mech. **210**, 155 (1990).
[14] A. Oron, S. H. Davis, and S. G. Bankoff, "Long-scale evolution of thin liquid films," Rev. Mod. Phys. **69**, 931 (1997).
[15] J. Gratton and C. L. M. Vigo, "Evolution of self-similarity, and other properties of waiting-time solutions of the porous media equation: The case of viscous gravity current," Eur. J. Appl. Math. **9**, 327 (1998).
[16] G. I. Barenblatt and Y. B. Zel'dovich, "Self-similar solutions as intermediate asymptotics," Annu. Rev. Fluid Mech. **4**, 285 (1972).
[17] F. Brochard-Wyart, H. Hervet, C. Redon, and F. Rondelez, "Spreading of heavy droplets. I. Theory," J. Colloid Interface Sci. **142**, 518 (1991).

[18]M. Brenner and A. Bertozzi, "Spreading of droplets on a solid surface," Phys. Rev. Lett. **71**, 593 (1993).
[19]J. A. Diez, R. Gratton, L. P. Thomas, and B. Marino, "Laplace pressure-driven drop spreading: Quasi-self-similar solution," J. Colloid Interface Sci. **168**, 15 (1994).
[20]R. Gratton, J. A. Diez, L. P. Thomas, B. Marino, and S. Betelú, "Quasi-self-similarity for wetting drops," Phys. Rev. E **53**, 3563 (1996).
[21]M. Bertsch, R. Dal Passo, S. H. Davis, and L. Giacomelli, "Effective and microscopic contact angles in thin film dynamics," Eur. J. Appl. Math. **11**, 181 (2000).